Manufacturing Letters 41 (2024) 28–32

Contents lists available at ScienceDirect

Manufacturing Letters

journal homepage: www.elsevier.com/locate/mfglet

Letters

Experimental identification of yield surface for additively manufactured stainless steel 316L under tension–compression-torsion conditions considering its printing orientation

Mateusz Kopec [a,*], Ved Prakash Dubey [a], Marzena Pawlik [b], Paul Wood [b], Zbigniew L. Kowalewski [a]

[a] Institute of Fundamental Technological Research, Polish Academy of Sciences, Pawinskiego 5B, Warsaw 02-106, Poland
[b] Institute for Innovation in Sustainable Engineering, College of Science and Engineering, University of Derby, DE22 1GB, UK

ARTICLE INFO

Article history:
Received 20 March 2024
Received in revised form 7 June 2024
Accepted 10 July 2024
Available online 5 August 2024

Keywords:
Stainless steel
Yield surface
Additive manufacturing
Laser Powder Bed Fusion Melting (LPBF-M)

ABSTRACT

Stainless steel 316L tubes and bars were additively manufactured (AM) by using the Laser Powder Bed Fusion Melting (LPBF-M) method in three orientations. As-built specimens were then machined and the initial yield surface was determined for three printing orientations based on the yield stress definition for 0.005 % plastic offset strain. The as-received, wrought material was additionally tested using the same tension–compression-torsion conditions to compare the mechanical behaviour of AM and wrought SS316L. The sizes of yield surfaces elaborated for LPBF-M specimens increased along the tensile and compressive directions and shrunk when torsion was applied, as compared to the as-received specimen.

1. Introduction

SS316L is extensively utilized across various industrial sectors due to the excellent combination of mechanical properties, corrosion resistance, weldability, and formability [1]. Additionally, SS316L is recognized for its low thermal conductivity, high melting point, limited sensitivity to oxygen absorption, and high absorptivity in infrared, making it an exceptional material for AM [2]. AM for SS316L encompasses different technologies such as Powder Bed Fusion (PBF), Directed Energy Deposition (DED), Fused Deposition Modeling (FDM), and Binder Jetting (BJ) [3]. The selection of the appropriate printing technology and parameters is crucial for ensuring a successful process during which crack-free components with extremely low porosity can be manufactured [4]. Therefore, it is essential to apply optimized process parameters to achieve the required mechanical properties [5] since they are strongly dependent on the AM process strategy applied. Uniaxial tensile tests conducted on SS316L manufactured using Selective Laser Melting (SLM) [6], Directed Laser Deposition (DLD) [7], Laser Engineered Net Shaping (LENS) [8], and High-Power Direct Laser Deposition [9] have demonstrated superior properties in the horizontal and 45° orientations compared to the vertical orientation. One should stress, that uniaxial testing provides only limited data on the anisotropy of AM SS316L, which is insufficient to fully understand all aspects of its behaviour, especially when different printing orientations are applied. In order to expand the knowledge of the mechanical behaviour of AM SS316L, the yield surface concept could be used. An interior of the yield surface can be described as a region in the stress space where the material always behaves as elastic. Hence, an experimental identification of such surfaces would be extremely important since it provides realistic stress values under which material could operate without permanent deformation. Unfortunately, the available literature on the experimental identification of yield surface for additively manufactured stainless steel 316L is still limited. Somlo et al. [10] presented a computing attempt to determine yield surfaces for additively manufactured metals, austenitic stainless steel 316L and titanium alloy Ti-6Al-4 V, through crystal plasticity modelling [10]. Although some experimental papers could be found on the identification of yield surface based on the uniaxial tensile and biaxial tensile behaviour of the 316L stainless steel manufactured by selective laser melting, they are not considering printing orientation [11,12].

The experimental studies on yield surface identification for AM materials are also important from the modelling point of view. In the last decade, crystal plasticity has become an indispensable tool for establishing a connection between the microstructure of materials and their macroscopic mechanical strength [10]. It allows for a detailed description of the plastic deformation mechanisms of different AM materials including SS316L. It should be stressed, that

* Corresponding author.
E-mail address: mkopec@ippt.pan.pl (M. Kopec).

https://doi.org/10.1016/j.mfglet.2024.07.003

despite having the same chemical composition, such material exhibits distinct mechanical properties as compared to its wrought form [1,2,7–9]. Therefore, it is of the highest importance to reveal the deformation mechanisms to further implement them into the material model to precisely predict its behaviour. At larger scales, the heterogeneous microstructure of AM metals can be described using a homogeneous elastic–plastic material model [10]. An anisotropic yield function is usually employed to govern the plastic behaviour, and it can be determined through crystal plasticity simulations or directly from the experiments. There are numerous anisotropic yield criteria available, each utilizing quadratic or non-quadratic yield functions with varying numbers of adjustable parameters. Generally, the complexity and flexibility of a yield function increase with the number of parameters it incorporates. However, calibrating multiple parameters requires extensive experimental testing.

Therefore, the main aim of this paper is to experimentally determine an initial yield surface of AM SS316L for three printing orientations based on the yield point definition in form of the plastic offset strain equal to 0.005 %. Subsequently, a comparison of the yield surface determined for wrought material was performed to assess a suitability of the proposed LPBF-M methodology in manufacturing of the material having similar characteristics as the wrought one.

2. Materials and methods

The round bars and tubes of diameter and length equal to 13 mm and 70 mm, respectively, were additively manufactured by using the Renishaw AM 250 system and the SS316L powder feedstock supplied by the same company. They were printed in three directions (Z – vertical, XY – horizontal, ZX – 45°) (Fig. 1a) applying the process parameters presented in Table 1.

After the AM process, the as-built specimens were subjected to stress relief using a 470 °C soak for 6 h whilst still attached to the build plate following standards. The bars were then wire cut from the build plate and subsequently machined to achieve the specimen geometry illustrated in Fig. 1b. Both, the inner and outer surfaces of the specimens were machined using the same turning parameters. Mechanical tests were performed on the MTS 858 servo-electrohydraulic biaxial testing machine with the maximum capacity of ± 25kN axial force and ± 100 Nm torque at room temperature (23 °C). At the beginning of the experimental program, the uniaxial tensile test was carried out to determine the basic properties of the material including the conventional yield strength (YS) $R_{0.2}$. Based on the stress–strain characteristic, the definition of yield point for 0.005 % plastic offset strain was determined. Since a single specimen approach was used in this work, such a small plastic offset strain for the definition of yield can be used to determine the yield surface as the accumulation of additional plastic strain from the previous loading path was negligible. Therefore, considering the cost perspective of the experiment and to provide a more realistic elastic-to-plastic transition, 0.005 % plastic offset strain definition of yield for all the yield surfaces was adopted. For the purpose of subsequent experiments, Vishay 120 Ω strain gages were bonded in the middle of outer surface of gauge section of the thin-walled tubular specimens to measure and control axial, shear and hoop strain components (Fig. 1c). During yield probing, the axial and shear strain components were measured by using three-element 45° rectangular rosette EA-05-125RA-120 while for the hoop strain, linear pattern rosette EA-13-062AK-120 was used. A detailed description of the methodology implemented for the precise strain measurement and control of tests was presented in [13]. A single specimen approach and sequential probing technique under strain-controlled loading were used to determine an initial yield surface for each state of the material (as-received and three printing orientations) involving 17 distinct stress paths. The sequence commenced under tension and finished with tension in the same direction within the $(\varepsilon_{xx}, \sqrt{(3/(1+\nu)^2)}\varepsilon_{xy})$ strain plane (Fig. 1d), where ν is Poisson's ratio. Loading for each path began from the origin and continued until a limited plastic offset strain of 1.5 x 10^{-4} (0.015 %) was achieved. Then, the stress-controlled unloading process was executed until the force and torque reached zero values. The yield points were identified through the designated offset strain technique, where yield is determined as the point at which the equivalent stress–strain curve deviates by 0.005 % from the elastic line in each loading direction. The Szczepinski anisotropic yield condition was utilized for the numerical computation of the yield surface [14]. The experimental yield points were fitted with the Szczepinski anisotropic yield equation using the least squares method.

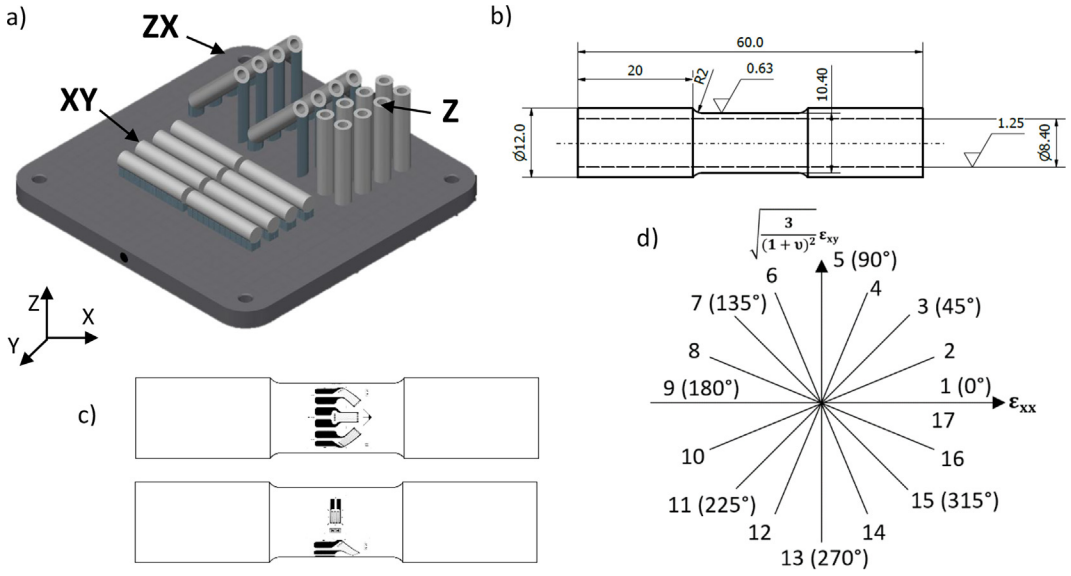

Fig. 1. Printing orientation of specimens on the build plate (a); engineering drawing of the tubular specimen for yield surface determination (b); schemes of the strain gauge circuits on the specimen (c); loading sequence of strain paths for yield points determination in the biaxial strain space (d).

Table 1
Process parameters applied during AM.

Region	Layer thickness [μm]	Hatch distance [mm]	Beam Comp [mm]	Focal point [mm]	Power [W]	Point distance [μm]	Exposure time [μs]	Scan speed [mm/s]	Energy density [J/mm^3]
Volume Fill	50	0.11	0.025	0	195	60	80	750	47.27
Hatch									
Scanning strategy	Meander								

3. Experimental results and discussion

Firstly, the tubular specimens were subjected to uniaxial tensile tests to determine the yield strength, ultimate tensile strength, elongation and Young modulus (Fig. 2a, Table 2). The results obtained were similar to those documented in [6] for the same SLM process and various printing orientations, as well as for components manufactured using LENS [8]. Previous studies [15] have shown, that the elongation of SLM SS316L in the Z direction can exceed 20 % depending on the heat treatment, with higher variability observed in the Z direction compared to the XY plane. It is widely acknowledged that the mechanical properties of AM SS316L are influenced by the level of anisotropy. The difference in strength has been linked to the printing orientation [9]. When SS316L is printed horizontally, the loading direction aligns parallel to the sliced layers, with the scanning tracks acting as reinforcing fibres within the material [9]. Conversely, in the vertical direction, the loading orientation is perpendicular to the sliced layers, resulting in weaker metallurgical bonds between layers and consequently lower tensile properties.

Subsequently, the stress–strain dependence for each state of the material was investigated in each of the 17 distinct stress paths in a narrow strain range to determine the yield points for further calculations of the yield surface. The representative results for direction 0 was presented in Fig. 2b. It was found, that the sizes of yield surfaces elaborated for LPBF-M specimens increased along tensile and compressive directions and shrunk in directions where torsion was applied, as compared to the specimen in wrought, as-received conditions (Fig. 2c). Such behaviour was probably associated with material anisotropy, and thus, different textures [16] and crystal structures [10]. The main ellipse parameters for the determined yield surfaces of SS316L manufactured in three orientations as well as for the as-received material were presented in Table 2. Since the yield surface axis ratios of the printed materials are lower than the same ratio for an isotropic material according to the Huber-von Mises yield condition (1.73), an occurrence of some initial anisotropy was confirmed. The shape of yield surfaces for all printing orientations strongly indicates the texture presence [17]. However, it could be observed, that the specimen built in the Z orientation exhibits a notable shift in the compression direction in comparison

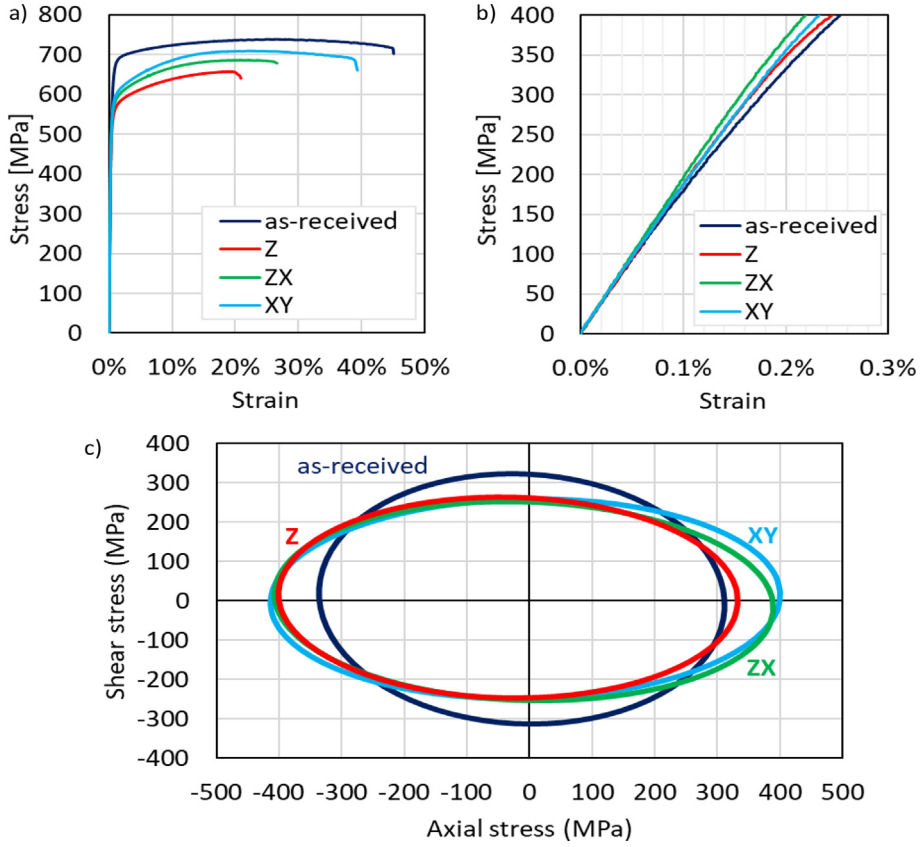

Fig. 2. Standard tensile characteristics of the additively manufactured and as-received SS316L (a) and the same curves presented for limited strain range (b); comparison of the yield surfaces for three printing orientations and the same material in the as-received state for 0.005 % plastic offset strain (c).

Table 2
The mechanical properties and ellipse parameters for the initial yield surfaces of wrought and AM SS316L.

	σ_y [MPa]	σ_{UTS} [MPa]	A [%]	E [GPa]	Centre $(\boldsymbol{x}_0, \boldsymbol{y}_0)$ [MPa]	Rotation angle () [Radian]	Semi-axes $(\boldsymbol{a}, \boldsymbol{b})$ [MPa]	Axes ratio $(\boldsymbol{a}/\boldsymbol{b})$
As-received	610	740	45	178	−12.63, 5.83	−0.61	329.11, 312.65	1.05
XY	553	713	40	182	−7.20, 4.25	0.04	407.19, 254.15	1.60
ZX	540	685	25	193	−8.32, −1.39	−0.07	398.93, 251.89	1.58
Z	505	660	22	185	−34.05, 7.60	−0.04	367.12, 255.28	1.44

to that representing the wrought material. It should be emphasised, that the anisotropic character of mechanical properties in AM SS316L is directly attributed to texture. It was reported, that desirable texture formation of (1 1 0) in the SLM-manufactured SS316L was observed to be located along the build direction [18], which corresponds to the Z orientation [19,20]. Therefore, the mechanical response of the specimen in Z orientation was significantly influenced by texture (Fig. 2a,c), while such a phenomenon was not observed for XY and ZY.

Considering the differences in mechanical properties due to the intrinsic anisotropy at different printing orientations, one should indicate the undoubtful effects of microstructure, melt pool, and temperature gradient that are directly related to such issues. Recent studies by Liu et al. [21] have shown, that a depth of the melt pool and remelting time interval can effectively control the grain size and dislocation density of SS316L manufactured by using dual-laser powder bed fusion. With the adoption of a 50 ms time interval, an increase of about 43 MPa in ultimate tensile strength could be achieved. During the LPBF-M process, the overlap of melt track boundaries could be found. The occurrence of such partial remelting between subsequent scanning tracks leads to the creation of a melting trajectory that exceeds the size of the laser spot due to the penetration depth being larger than the layer thickness [22]. Consequently, there is a remelting of the previous layer. This phenomenon enables grain growth in parallel or perpendicular orientations to the build direction in different dimensions, contributing to the anisotropic mechanical property [22,23]. Furthermore, it has been observed, that columnar grains grow in the direction of the temperature gradient, which also may affect the mechanical response of material when it is deformed along the printing orientation.

Although the yield surface concept is commonly known, the experimental identification of yield surfaces for additively manufactured materials can be treated as a relatively new approach used in mechanics to characterise the material behaviour subjected to complex loading in stress states separating the elastic and plastic ranges [16,24,25]. One should emphasize, that research in this area is mainly limited to numerical investigations through crystal plasticity [16,24] and anisotropic [25,26] models. Even though experimental data is used to validate or calibrate the model, it is mainly based on the uniaxial tensile test results. The approach presented by the authors is thus important as it provides the experimental data for AM SS316L for which the yield surfaces were determined for three different printing orientations. Future studies should involve the combination of numerical and experimental approaches to establish a new model, which could be validated through data obtained in this paper.

4. Conclusions

In this paper, a new approach for experimental identification of yield surface for additively manufactured stainless steel 316L was presented. The yield surfaces were determined for the material manufactured in three different orientations for the plastic offset strain equal to 0.005 %. Additionally, the as-received, wrought material was tested using the same conditions to identify the mechanical behaviour variations. A single specimen approach and sequential probing technique under strain-controlled loading were successfully employed to determine an initial yield surface for each state of the material, involving 17 distinct stress paths. It was observed that the main dimensions of yield surfaces for LPBF-M specimens were increased along tensile and compressive directions, and shrunk significantly when torsion was applied. Such behaviour was associated with a certain form of material anisotropy representing different textures and crystal structures.

CRediT authorship contribution statement

Mateusz Kopec: Writing – original draft, Visualization, Validation, Supervision, Project administration, Methodology, Investigation, Formal analysis, Data curation, Conceptualization. **Ved Prakash Dubey:** Investigation, Formal analysis, Data curation. **Marzena Pawlik:** Methodology, Investigation. **Paul Wood:** Writing – review & editing, Validation, Project administration, Methodology, Investigation, Formal analysis. **Zbigniew L. Kowalewski:** Writing – review & editing, Validation, Formal analysis.

Declaration of Competing Interest

The authors declare that they have no known competing financial interests or personal relationships that could have appeared to influence the work reported in this paper.

Acknowledgements

The authors would like to express their gratitude to Mr M. Wyszkowski and Mr. A. Chojnacki for their kind help during the experimental part of this work.

References

[1] Avanzini A. Fatigue Behavior of Additively Manufactured Stainless Steel 316L. Materials 2023;65:1–26. https://doi.org/10.3390/ma16010065.
[2] Bedmar J, Riquelme A, Rodrigo P, Torres B, Rams J. Comparison of different additive manufacturing methods for 316L stainless steel. Materials 2021;14:1–22. https://doi.org/10.3390/ma14216504.
[3] D'Andrea D. Additive Manufacturing of AISI 316L Stainless Steel: A Review. Metals 2023;13(8):1370. https://doi.org/10.3390/met13081370.
[4] Khalid M, Peng Q. Investigation of Printing Parameters of Additive Manufacturing Process for Sustainability Using Design of Experiments. J Mech Des 2021;143:32001. https://doi.org/10.1115/1.4049521.
[5] Santonocito D, Fintová S, Di Cocco V, Iacoviello F, Risitano G, D'Andrea D. Comparison on Mechanical Behaviour and Microstructural Features Between Traditional and AM AISI 316L. Fatigue Fract Eng Mater Struct 2023;46:379–95. https://doi.org/10.1111/ffe.13872.
[6] Alsalla HH, Smith C, Hao L. Effect of build orientation on the surface quality, microstructure and mechanical properties of selective laser melting 316L stainless steel. Rapid Prototyp J 2018;24:9–17. https://doi.org/10.1108/RPJ-04-2016-0068.
[7] Smith TR, Sugar JD, San Marchi C, Schoenung JM. Orientation Effects on Fatigue Behavior of Additively Manufactured Stainless Steel. Proceedings of the ASME 2017 Pressure Vessels and Piping Conference. Volume 6A: Materials and Fabrication. Waikoloa, Hawaii, USA. July 16–20, 2017. DOI: 10.1115/PVP2017-65948.
[8] Yang N, Yee J, Zheng B. Process-Structure-Property Relationships for 316L Stainless Steel Fabricated by Additive Manufacturing and Its Implication for Component Engineering. J Therm Spray Tech 2017;26:610–26. https://doi.org/10.1007/s11666-016-0480-y.

[9] Guo P, Zou B, Huang C, Gao H. Study on microstructure, mechanical properties and machinability of efficiently additive manufactured AISI 316L stainless steel by high-power direct laser deposition. J Mater Process Technol 2017;240:12–22. https://doi.org/10.1016/j.jmatprotec.2016.09.005.
[10] Somlo K, Frodal BH, Funch CV, Poulios K, Winther G, Hopperstad OS, et al. Anisotropic yield surfaces of additively manufactured metals simulated with crystal plasticity. Eur J Mech A Solids 2022;94:104506. https://doi.org/10.1016/j.euromechsol.2022.104506.
[11] Wang H, Shu X, Zhao J, et al. Biaxial tensile behavior of stainless steel 316L manufactured by selective laser melting. Sci Rep 2023;13:21925. https://doi.org/10.1038/s41598-023-49482-7.
[12] Kořínek M, Halama R, Fojtík F, Pagáč M, Krček J, Krzikalla D, et al. Monotonic tension-torsion experiments and FE modeling on notched specimens produced by SLM technology from SS316l. Materials 2021;14(1):33. https://doi.org/10.3390/ma14010033.
[13] Dubey VP, Kopec M, Łazińska M, Kowalewski ZL. Yield surface identification of CP-Ti and its evolution reflecting pre-deformation under complex loading. Int J Plast 2023;167:103677. https://doi.org/10.1016/j.ijplas.2023.103677.
[14] Szczepinski W. On deformation-induced plastic anisotropy of sheet metals. Archives of Mechanics 1993;45:3–38.
[15] Wood P, Libura T, Kowalewski ZL, Williams G, Serjouei A. Influences of horizontal and vertical build orientations and post-fabrication processes on the fatigue behavior of stainless steel 316l produced by selective laser melting. Materials 2019;12:4203. https://doi.org/10.3390/ma12244203.
[16] Charmi A, Falkenberg R, Ávila L, Mohr G, Sommer K, Ulbricht A, et al. Mechanical anisotropy of additively manufactured stainless steel 316L: An experimental and numerical study. Mater Sci Eng A 2021;799:140154. https://doi.org/10.1016/j.msea.2020.140154.
[17] Deepak Kumar, Gyan Shankar, K.G. Prashanth, Satyam Suwas, Control of texture and microstructure in additive manufacturing of stainless steel 316 L, Journal of Alloys and Compounds, 976, 2024, 173040 DOI: 10.1016/j.jallcom.2023.173040.
[18] Deepak Kumar, Gyan Shankar, K.G. Prashanth, Satyam Suwas, Texture dependent strain hardening in additively manufactured stainless steel 316L, Materials Science and Engineering: A, 820, 2021, 141483 DOI: 10.1016/j.msea.2021.141483.
[19] Chen J, Liu C, Dong K, Guan S, Wang Q, Zhang X, et al. Crystallographic orientation dependence of dynamic deformation behaviours in additively manufactured stainless steel. J Mater Res Technol 2023;24:6699–712. https://doi.org/10.1016/j.jmrt.2023.04.255.
[20] Sun S-H, Ishimoto T, Hagihara K, Tsutsumi Y, Hanawa T, Nakano T. Excellent mechanical and corrosion properties of austenitic stainless steel with a unique crystallographic lamellar microstructure via selective laser melting. Scr Mater 2019;159:89–93. https://doi.org/10.1016/j.scriptamat.2018.09.017.
[21] Liu Z, Yang Y, Xiao Y, Lei H, Yang C, Liu Z, et al. Investigation of 316L microstructure evolution mechanism and mechanical properties in dual-laser powder bed fusion with controllable remelting time interval. Mater Des 2024;239:112761. https://doi.org/10.1016/j.matdes.2024.112761.
[22] Wang J, Zhu R, Liu Y, Zhang L. Understanding melt pool characteristics in laser powder bed fusion: An overview of single- and multi-track melt pools for process optimization. Advanced Powder Materials 2023;2(4):100137. https://doi.org/10.1016/j.apmate.2023.100137.
[23] Iqbal N, Jimenez-melero E, Ankalkhope U, Lawrence J. Microstructure and Mechanical Properties of 316L Stainless Steel Fabricated Using Selective Laser Melting. MRS Adv 2019;1–9. https://doi.org/10.1557/adv.2019.251.
[24] S. Amir H. Motaman, Franz Roters, Christian Haase, Anisotropic polycrystal plasticity due to microstructural heterogeneity: A multi-scale experimental and numerical study on additively manufactured metallic materials, Acta Materialia, 185, 2020, 340-369, DOI: 10.1016/j.actamat.2019.12.003.
[25] Agius D, Wallbrink C, Kourousis KI. Efficient modelling of the elastoplastic anisotropy of additively manufactured Ti-6Al-4V. Addit Manuf 2021;38:101826. https://doi.org/10.1016/j.addma.2020.101826.
[26] Wilson-Heid AE, Qin S, Beese AM. Anisotropic multiaxial plasticity model for laser powder bed fusion additively manufactured Ti-6Al-4V. Mater Sci Eng A 2018;738:90–7. https://doi.org/10.1016/j.msea.2018.09.077.